

Journal of Biomedical Optics

SPIDigitalLibrary.org/jbo

Reflected light intensity profile of two-layer tissues: phantom experiments

Rinat Ankri
Haim Taitelbaum
Dror Fixler

Reflected light intensity profile of two-layer tissues: phantom experiments

Rinat Ankri,^{a,b} Haim Taitelbaum,^b and Dror Fixler^a

^aBar Ilan University, School of Engineering and the Institute of Nanotechnology and Advanced Materials, Ramat Gan, 52900, Israel

^bBar-Ilan University, Department of Physics, Ramat Gan, 52900, Israel

Abstract. Experimental measurements of the reflected light intensity from two-layer phantoms are presented. We report, for the first time, an experimental observation of a typical reflected light intensity behavior for the two-layer structure characterized by two different slopes in the reflected light profile of the irradiated tissue. The point in which the first slope changes to the second slope, named as the crossover point, depends on the upper layer thickness as well as on the ratio between the absorption coefficients of the two layers. Since similar experiments from one-layer phantoms present a monotonic decay behavior, the existence and the location of the crossover point can be used as a diagnostic fingerprint for two-layer tissue structures. This pertains to two layers with greater absorptivity in the upper layer, which is the typical biological case in tissues like skin. © 2011 Society of Photo-Optical Instrumentation Engineers (SPIE). [DOI: 10.1117/1.3605694]

Keywords: reflected light intensity measurements; phantom experiments; biological structures; two-layer tissues; photon migration.

Paper 11059RRR received Feb. 8, 2011; revised manuscript received Jun. 4, 2011; accepted for publication Jun. 7, 2011; published online Aug. 4, 2011.

1 Introduction

Light-tissue interaction has been investigated for various applications in medicine. In the diagnostic field, one can get information about the structure and the physiological function of the irradiated tissue from the profile of the transmitted or re-emitted light. Changes in the spectrum and the intensity of the light, compared to the injected light, result from interactions of the irradiated light with the tissue components.^{1,2}

Several optical imaging techniques, such as X-ray computed tomography (X-ray CT),³ two-photon microscopy,⁴ photoacoustic imaging (PAI),⁵ and optical coherence tomography (OCT)⁶ are widely utilized in the medical diagnosis field. Each of these techniques measure a different physical property and has resolution and penetration depth that prove advantageous for specific applications. Although X-ray CT can be used to image bodily structure at relatively high spatial resolution, it does so using ionizing radiation with its associated patient risk.⁷ The two-photon microscopy and OCT are highly successful and safe but none of these technologies can provide penetration beyond ~1 mm into scattering biological tissues since the optical scattering in soft tissues significantly degrades spatial resolution with depth.⁸ The PAI does penetrate most biological tissues for depths greater than 1 mm but it is more complicated to use. Among these sophisticated optical methods, reflectance spectroscopy is a simple, safe, and easy-to-apply diagnostic technique that has the potential to provide important basic morphological information about biological tissue without requiring high penetration depth.

Several models for the analysis of the reflected light intensity from biological tissues were developed during the last decades.⁹⁻¹¹ Most of these models refer to one layer tissues,

in which the entire tissue can be described by a single set of absorption and scattering coefficients. These models provide theoretical tools for tissue optical properties investigation and some of them were combined with experimental validation of the theoretical expressions.¹²⁻¹⁵ Nevertheless, the more realistic case is the layered characterization, which corresponds to most biological tissues such as stomach, skin, brain, and more.^{16,17} Therefore, several two-layer and multilayered models have been developed.¹⁸⁻²³ These models present theoretical results for light path within layered tissues and some of them strengthen the theoretical approaches by phantom experiments.^{10,24-26} Still, none of these works has presented experimental results that can clearly distinguish between the reflected light intensity profile of one-layer and two-layer tissues. Schmitt et al.¹⁶ has presented some results of the reflected light intensity from two-layer phantom, as well as from *in vivo* measurements of skin tissue, but the potential theoretical tools were not employed.

One of the most simplest tools for layered tissue investigation was proposed by Nossal et al., which presented a random walk theory for light path within layered tissues.¹⁸ In this paper, the injected photons travel within a two-layer tissue structure and the re-emitted intensity profile, $\Gamma(\rho)$ (with ρ as the light source-detector separation, see Fig. 1), is theoretically analyzed for optical properties diagnosis. First, they showed that when the absorptivity of the bottom layer is greater than the absorptivity in the upper layer, there is no evidence whatsoever for a two layer structure, as the profile exhibits a single-layer behavior, albeit with an effective average absorptivity. In the opposite case, when the upper absorptivity is greater, the predicted profile exhibits two different slopes, representing the reflected light behavior according to photons arriving from the upper and the bottom layer, respectively. Based on this random walk approach, Taitelbaum et al. provided a theoretical expression for the

Address all correspondence to: Haim Taitelbaum, Bar Ilan University, Department of Physics, Ramat Gan, 52900, Israel; Tel: 972-3-5318465; Fax: 972-3-7384054; E-mail: haimt@mail.biu.ac.il.

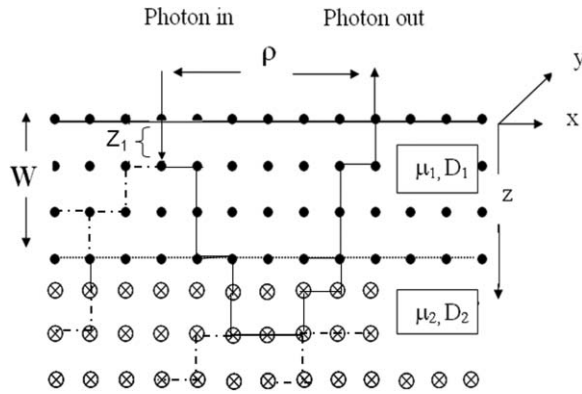


Fig. 1 Schematic description of a photon trajectory in a two-layer lattice. The light source-detector separation is ρ and the upper layer thickness is W . The solid line presents the trajectory of a reflected photon that arrived to the detector and the dotted lines are the trajectories of the absorbed photons. μ_1 and μ_2 are the upper and bottom-layer absorption parameters in the random-walk model. D_1 and D_2 are the diffusion coefficients and z_1 is the characteristic scattering length of the tissue in the diffusion model.

reflected light intensity profile of this kind of a two-layer tissue,¹⁹ supported by simulations only. A similar theoretical result was also proposed by Dayan et al., which used the diffusion theory for the description of light path within a two-layer tissue.²⁰ Both, Taitelbaum et al. and Dayan et al. presented a “broken” curve for the re-emitted intensity from such a two-layer tissue (with large enough upper layer thickness), different from the monotonic decay of the reflected light intensity from a homogeneous, one-layer tissue⁹ (and two-layers with greater absorptivity in the bottom). The value of ρ , the light source-detector separation, corresponding to the crossover between the two slopes was named as “the crossover point” and was symbolized as ρ_c . Both, Taitelbaum et al. and Dayan et al., suggested that ρ_c linearly depends on the upper layer thickness. In the random walk theory the crossover point is given by¹⁹

$$\rho_c \approx W \left[1 + \sqrt{\mu_2/\mu_1} \right], \quad (1)$$

where μ_1 and μ_2 are the absorption parameters of the upper and bottom layers, respectively, and W is the upper layer thickness. In the diffusion theory,²⁰ the crossover point is given as

$$\rho_c \approx \frac{2W}{z_1(\theta_1 - \theta_2)}, \quad (2)$$

where θ_1 and θ_2 are parameters that depend on the upper and bottom layer absorption parameters (μ_1 and μ_2) and diffusion coefficients (D_1 and D_2), and z_1 is the characteristic scattering length of the tissue²⁰ as illustrated in Fig. 1.

These theoretical approaches were substantiated by simulations.^{19,20} About a decade later, in 1998, a similar simulated profile was presented by Alexandrakis et al.,²¹ with a crossover point in the reflected intensity profile from two-layer tissues, also based on the diffusion theory for light path within the layered tissue.

However, so far no experimental validation for this crossover point and its dependence on the upper layer width has been obtained, and its existence was merely a theoretical prediction.

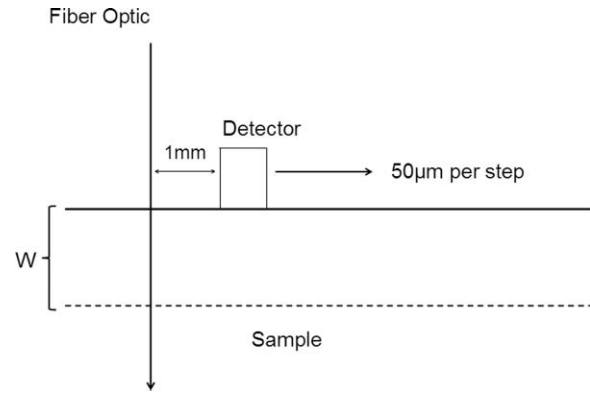


Fig. 2 Schematic description of the experimental setup for linear reflected light intensity measurements. The laser diode wavelength was 650 nm and an optic fiber (arrow) was used to enable the sample irradiation on a single point on its surface. The photodiode was in close contact with the phantom surface. The micrometer plate was moved 60 steps of 50 μm each, enabling continuous measurements of the spatial reflectance from the phantom from 1 mm up to 4 mm from the laser diode position.

Therefore, an experimental validation for the crossover point is highly important.

In this paper, experimental results of the reflected light intensity profiles from different two-layer phantoms are presented. The aim of the current study is to experimentally test whether reflected light intensity measurements can indeed be used as a diagnostic tool that distinguishes between one-layer and two-layer tissue structures, based on the crossover point fingerprint in two-layer tissues with higher absorptivity in the upper layer. The crossover point dependence on the phantom optical properties was investigated as well.

In Sec. 2, we describe the materials and methods of our measurement system. In Sec. 3, we present the experimental results. Section 4 concludes the paper.

2 Materials and Methods

2.1 Experimental Setup

A noninvasive optical technique was designed and built (NEGOH-OP Technologies, Israel) for reflected light intensity measurements (see Fig. 2). The setup included a laser diode, as an excitation source, with a wavelength of 650 nm. The choice of this wavelength is due to its large usage in the medical field, such as LLLT treatments^{27,28} and PPG measurements²⁹ and due to its proximity to the NIR region (which is the relevant optical region for the photon migration model⁹). The irradiation was carried out using an optic fiber with a diameter of 125 μm . As a photo detector, we used a portable photodiode that was deposited in different distances ρ on the sample surface in order to enable $\Gamma(\rho)$ measurements. The photodiode had a cross-section diameter of 1 mm². The initial distance ρ between the light source and the first photodiode was ~ 1 mm. A consecutive reflected light intensity measurement was enabled using a micrometer plate on which the phantom was deposited. The micrometer plate was moved for 60 steps of 50 μm each. Thus, the reflected light intensity was collected from ~ 60 source-detector distances with ρ varying between 1 mm (the initial distance between the light source and the

Table 1 Optical properties of the irradiated two-layer phantoms. The concentration of IL refers to the fraction of solids in the solution, while the concentration of ink pertains to the fraction of the original product.

Phantom #	Optical properties [mm ⁻¹]	Ink concentration [%]	IL concentration [%]
1	$\mu_1 = 0.0192, \mu_{S_1} = 0.8$	6×10^{-3}	0.8
	$\mu_2 = 0.0064, \mu_{S_2} = 0.8$	2×10^{-3}	0.8
2	$\mu_1 = 0.0192, \mu_{S_1} = 0.8$	3×10^{-3}	0.8
	$\mu_2 = 0.0064, \mu_{S_2} = 1.2$	2×10^{-3}	1.2
3	$\mu_1 = 0.0096, \mu_{S_1} = 1.2$	3×10^{-3}	1.2
	$\mu_2 = 0.0096, \mu_{S_2} = 0.8$	3×10^{-3}	0.8
4	$\mu_1 = 0.0192, \mu_{S_1} = 0.8$	6×10^{-3}	0.8
	$\mu_2 = 0.0096, \mu_{S_2} = 0.8$	3×10^{-3}	0.8
5	$\mu_1 = 0.0096, \mu_{S_1} = 0.8$	3×10^{-3}	0.8
	$\mu_2 = 0.0056, \mu_{S_2} = 0.8$	1.7×10^{-3}	0.8
6	$\mu_1 = 0.0096, \mu_{S_1} = 0.8$	3×10^{-3}	0.8
	$\mu_2 = 0.0064, \mu_{S_2} = 0.8$	2×10^{-3}	0.8
7	$\mu_1 = 0.0096, \mu_{S_1} = 0.8$	3×10^{-3}	0.8
	$\mu_2 = 0.0073, \mu_{S_2} = 0.8$	2.2×10^{-3}	0.8

photodiode) and the maximal ρ was ~ 4 mm. A schematic description of the measurements procedure is presented in Fig. 2.

The reflected intensity $\Gamma(\rho)$, presenting units of Volts, was collected using a digital scope (Agilent Technologies, Mso7034a, Santa Clara, California) and the data was processed using MATLAB.

2.2 Irradiated Sample

Solid phantoms, with different absorption coefficients, were prepared in order to simulate a skin tissue with different optical properties.³⁰ The phantoms were prepared using varying concentrations of Indian ink 0.1%, as an absorbing component, Intralipid 20% (Lipofundin MCT/LCT 20%, B. Braun Melsungen AG, Germany) as a scattering component³¹ and Agarose powder (SeaKem, LE Agarose, Lonza, USA), in order to convert the solution into gel. The absorption spectrum of the Indian ink was determined using a spectrophotometer and the absorption coefficient, symbolized as μ , of each phantom was calculated according to the concentration of the ink in each solution. The reduced scattering coefficients, $\mu_{S'}$, of the phantoms were calculated using the Mie theory.³² The two layer phantoms were prepared as follows: first, the bottom layer solution, which was prepared with ink and IL concentrations corresponding to the lower layer parameters, was prepared and solidified in vacuum conditions. Then, the upper layer solution that was similarly prepared corresponding to the upper layer parameters was poured and solidified on the bottom layer.

The phantoms were prepared in cell culture plates (90 mm) and were cooled in vacuum conditions (to avoid bubbles). Several different two-layer phantoms were prepared and their optical properties at 650 nm were chosen according to skin optical properties presented by Dam et al.³⁰ The phantoms' optical properties are presented in Table 1.

All phantoms present the required condition for a two-layer tissue structure to exhibit the crossover behavior.¹⁹ Each phantom had a very thin upper layer thickness (up to 1 mm) with a bottom layer of 10 mm thickness. Thus, the bottom layer could be considered as an infinite layer compared to the upper layer.^{19,20}

3 Results

3.1 Crossover Point in the Reflectance from Two-layer Phantoms

Figure 3(a) presents the reflectance measured from phantom #1 (see Table 1) with an upper layer thickness of $W = 0.7 \pm 0.1$ mm (the thick solid lines). The reflected light intensity profiles from two one-layer phantoms with absorption coefficients equal to $\mu_1 = 0.0192$ mm⁻¹ and $\mu_2 = 0.0064$ mm⁻¹ are also presented (the dotted and thin solid lines, respectively) for comparison. The reflected light intensity profile of the two-layer phantom presents a crossover point between two different slopes, while the one-layer phantoms present a monotonic decay. The first slope (the slope prior to the crossover point) is equal to the slope of the one-layer phantom with absorption coefficient μ_1 , suggesting that in short distances the contribution is due to

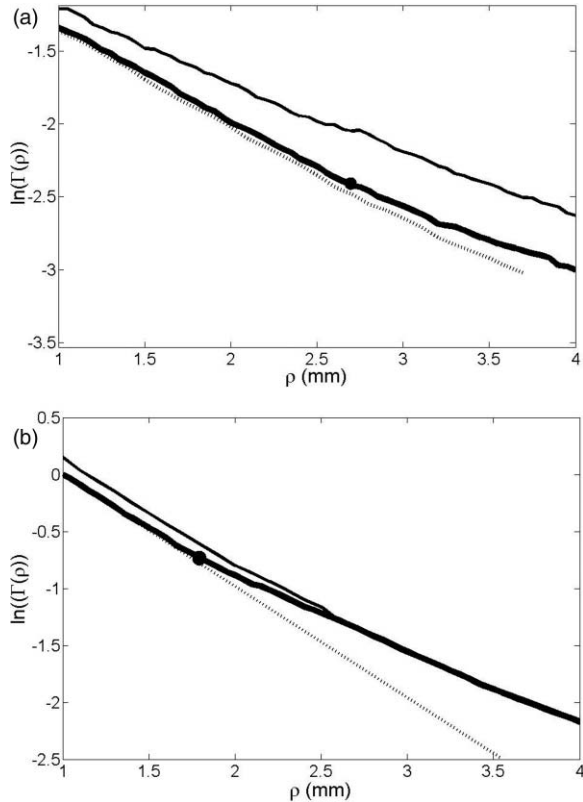


Fig. 3 Crossover point in the reflected light intensity profile of two-layer phantoms (thick solid line) compared to the reflectance from two one-layer phantoms with the absorption and scattering coefficients μ_1 , $\mu_{s'1}$ (dotted line) and μ_2 , $\mu_{s'2}$ (thin solid line). (a) phantom #1 (Table 1) with $W = 0.7 \pm 0.1$ mm and (b) phantom #2 (Table 1) with $W = 0.5 \pm 0.1$ mm.

photons arriving from the upper layer of the phantom as was theoretically predicted.¹⁹ The second slope (the slope after the crossover point) is equal to the slope of the one-layer phantom with the absorption coefficient μ_2 , suggesting that the reflected intensity in the long distances is due to photons arriving after long trajectories in the bottom layer. The intersection of the two slopes determined the crossover point. This procedure has been performed for all the phantoms in our study.

Figure 3(b) presents the reflected light intensity from phantom #2 (the thick solid line) compared to the reflectance from one-layer phantoms with the same optical properties as for μ_1 and μ_2 (dotted and thin solid lines, respectively). In this phantom, both absorption and scattering coefficients of the two layers were different. The crossover point was also observed in the reflectance of phantom #3 (data not shown), which presents the same absorption coefficients for both layers but different scattering coefficients.

3.2 ρ_c Dependence on the Upper-Layer Thickness

Both theory^{18–20} and simulation^{19,20} predict that the thicker W is, the larger ρ_c is. Figure 4(a) shows the reflectance measured from a two-layer phantom (the thick solid line), which owns the same optical properties as in Fig. 3(a) but with an upper layer thickness of 0.3 ± 0.1 mm. The reflected light intensity profiles from two one-layer phantoms with optical

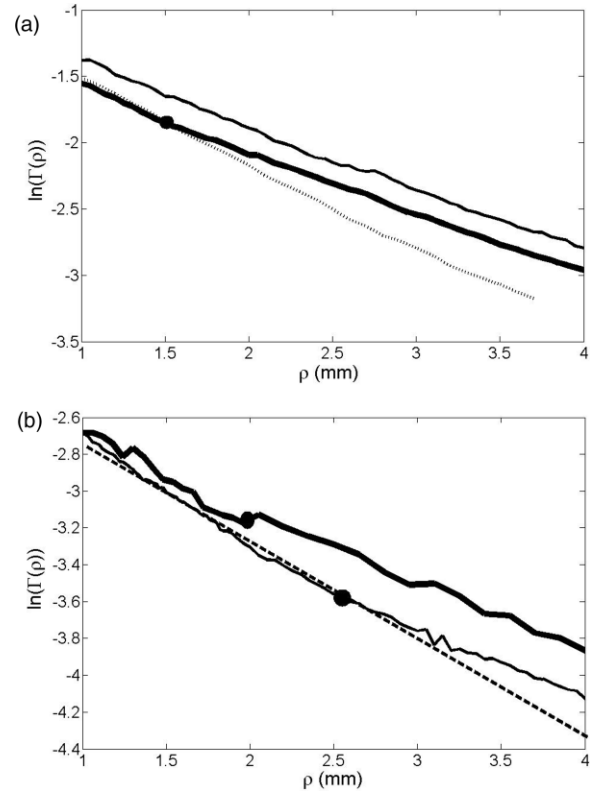


Fig. 4 Dependence of ρ_c on W : the reflected light intensity as a function of the distance ρ from (a) two-layer phantoms with same absorption coefficients as at Fig. 3 but with $W = 0.3 \pm 0.1$ mm; and (b) two two-layer phantoms with optical properties as phantom #4 from Table 1 with different upper layer thicknesses: $W = 0.8$ mm (thin solid line) and $W = 0.4$ mm (thick solid line). The measured reflectance profiles are compared to the reflectance from a one-layer phantom with an absorption coefficient μ_1 (dashed line).

properties μ_1 and μ_2 are also presented (dotted and thin-solid lines, respectively). The crossover point in the reflectance from the two-layer phantom is well seen. The comparison between Figs. 3(a) and 4(a) indicates that the crossover point location ρ_c depends on W : the thicker W is, the larger ρ_c is. While phantom #1, with an upper layer thickness of 0.7 ± 0.1 mm, presented $\rho_c = 2.7 \pm 0.05$ mm [Fig. 3(a)], phantom #2 [Fig. 4(a)], with $W = 0.3 \pm 0.1$ mm, presented $\rho_c = 1.55 \pm 0.05$ mm.

Similar results were observed for phantom #4. Two phantoms, differing by their upper layer thicknesses, were sampled. The reflected light intensity profiles from those phantoms are presented in Fig. 4(b). The decaying graphs clearly present the crossover point between the two slopes and the dependence of ρ_c on W is also well noticed: the upper layer thicknesses (W) were 0.4 ± 0.1 and 0.8 ± 0.1 mm and ρ_c presents 2 ± 0.05 and 2.5 ± 0.05 mm, respectively.

3.3 ρ_c Dependence on the Ratio μ_1/μ_2

As presented in the introduction by Eq. (1), ρ_c depends not only on the upper layer thickness but also on the square root of the ratio between the absorption parameters of the bottom and upper layers. Let us define R to be the ratio between μ_1

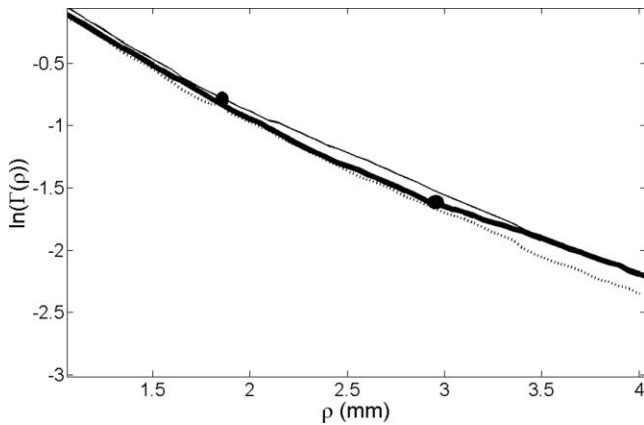


Fig. 5 Dependence of ρ_c on μ_1/μ_2 : the reflected light intensity profile of two-layer phantoms #2 and #5 from Table 1, thus, $\mu_1/\mu_2 = 3$ and 1.7 (thin and thick solid lines, respectively). The crossover points are clearly observed. However, in phantom #7 ($\mu_1/\mu_2 = 1.3$, dotted line), no crossover can be observed.

and μ_2 ($R \equiv \mu_1/\mu_2$): the smaller this R is, the larger ρ_c is. This dependence was experimentally tested, measuring the spatial reflectance from two-layer phantoms with different R . Figure 5 presents the reflected light intensity from phantom #2 (the thin solid line, presenting $R = 3$) and phantom #5 which has a relatively small value of $R = 1.7$ (thick solid line). The crossover point is still well noticed at the latter and ρ_c is relatively large: $\rho_c = 2.9 \pm 0.05$ mm. Similarly, the reflectance from phantoms #6 and #7, with the absorption coefficient ratios of $R = 1.5$ (data not shown) and $R = 1.3$ (dotted line in Fig. 5), was also measured. While the crossover point for phantom #6 was seen, a crossover point could not be seen by our experimental system for phantom #7.

These results strengthen the theoretical prediction for the dependence of ρ_c on the ratio between the absorption parameters: when $R \rightarrow 1$, the more similar are the reflectance slopes of the two layers, and the crossover point cannot be observed by using our experimental system.

4 Discussion

The dependence of the reflected light intensity profile on the tissue optical properties was intensively discussed.^{9,10,13,17,18} The analytical models of Taitelbaum et al.¹⁹ and Dayan et al.²⁰ suggested an identification of a two-layer tissue structure using reflected light intensity analyses.

In the present study, reflected light intensity measurements from two-layer phantoms are presented. Our experimental results verify the theoretical predictions: the reflectance profile presents a crossover point between two different slopes, corresponding to the two different absorption layers of the phantom. This might be a significant step forward, allowing one to use the theoretical models for diagnostic purposes of two-layer tissue structures.

Figure 3(a) presents the reflectance from two-layer phantoms with two absorption coefficients μ_1 and μ_2 for the upper and lower layers, respectively. The two different slopes were compared to the reflectance curves of two different one-layer phantoms with the same absorption coefficients of the upper

and bottom layers of the two-layer phantom, μ_1 and μ_2 , and were found to be the same. The physical phenomenon behind our experimental findings is that each layer of the two-layer tissue contributes reflected photons to different distances on the tissue surface.^{18,19} At small ρ (in our results about 2–3 mm) the measured intensity is mainly due to photons traveling in the upper layer only, meaning, in the absorption region of μ_1 . The intensity profile for large ρ (in our results: $\rho > 3$ mm) has a significant dependence on μ_2 due to the fact that most of the arriving photons have traveled through the lower layer.

Schmitt et al.¹⁶ presented the reflected light intensity from two-layer phantoms as well as from *in vivo* measurements of skin tissue. Their relevant experimental results (Figs. 9 and 10) clearly present two different slopes, but those two slopes were not discussed as a quantitative means for identifying a two-layer structure. Our experimental results for the reflectance from two-layer phantoms emphasize the crossover point in the reflected light intensity profile, as well as its dependence on W , as a practical diagnostic tool.

Both Taitelbaum et al. and Dayan et al. predicted a dependence of ρ_c on W and on the ratio μ_1/μ_2 . Figures 4(a) and 4(b) show that indeed the thicker W is, the bigger ρ_c is. The physical explanation for this finding is that the measured intensity for distances less than 3 mm is mainly due to photons that traveled in the upper layer only. As W increases, the extent of this single layer region also increases, therefore, the location of ρ_c increases as well.¹⁹ Further experimental investigation is required in order to substantiate the relation between ρ_c and W .

Figure 5 experimentally strengthens the dependence of ρ_c on μ_1/μ_2 : for relatively high values of R , such as $R = 3$, the crossover point presented in Fig. 5 is larger than the presented ρ_c in Figs. 3 and 4. This result demonstrates that the bigger μ_1/μ_2 is, the smaller the resulted ρ_c is, as predicted by Eq. (1). Schmitt et al.¹⁶ argued that the slope change occurs only for large differences at the absorptivities. Our results also present a crossover point for relatively small values of R , such as $R = 1.5$. It suggests that the crossover point can serve as a two-layer fingerprint even if the absorptivities difference is not so large.

Figure 3(b) presents the reflectance from a two-layer phantom presenting not only different absorption but also different scattering coefficients for its two layers. While the absorption was higher in the upper layer, the scattering presented a higher value in the bottom layer. As was suggested by Schmitt et al.,¹⁶ by increasing the scattering properties of the tissue, the reflectance slope becomes more sensitive to the absorption coefficient value. Therefore, one can define an effective coefficient, μ_{eff} , which depends on the product $\mu_s \mu_s'$.³³ Thus, despite the higher scattering in the bottom layer, the measured phantom presented a higher effective coefficient in the upper layer. Indeed, the resulted reflectance presents a well-noticed crossover point in the reflectance profile.

Different physiological conditions can be characterized by different optical properties. An example is a tumor, which has a different absorption coefficient than its surrounding³⁴ and can, therefore, be regarded as a separate layer within the tissue. As was suggested by Nossal et al.,¹⁸ the two-layer diffuse reflectance measurements can be used for some potential clinical applications involving tumor detection and therapy: when irradiating pigmented epithelia of a finite thickness, such as a region of malignant melanoma tissue,³⁴ one can reveal how the

underlying tissue layer affects the absorption profile. In order to avoid invasive measurements within the tissues, information may only be available from photons that penetrate and subsequently are re-emitted from the surface.¹⁸ Our results suggest that reflected light intensity measurements can indeed be used as a diagnostic tool for multi-layer tissue structure investigation.

References

1. R. A. J. Groenhuis, A. H. Ferwerda, and J. J. Ten Bosch, "Scattering and absorption of turbid materials determined from reflection measurements. 1: Theory," *Appl. Opt.* **22**, 2456–2462 (1983).
2. R. A. J. Groenhuig, J. J. Ten Bosch, and H. A. Ferwerda, "Scattering and absorption of turbid materials determined from reflection measurements. 2: Measuring method and calibration," *Appl. Opt.* **22**, 2463–2467 (1983).
3. G. N. Hounsfield, "Computerized transverse axial scanning (tomography): Part 1. Description of system," *J. Radiol.* **46**, 1016–1022 (1973).
4. W. Denk, J. Strickler, and W. Webb, "Two-photon laser scanning fluorescence microscopy," *Science* **248**, 73–76 (1990).
5. M. H. Xu and L. H. V. Wang, "Photoacoustic imaging in biomedicine," *Rev. Sci. Instrum.* **77**, 041101 (2006).
6. J. M. Schmitt, "Optical coherence tomography (OCT): a review," *IEEE J. Sel. Top. Quantum Electron.* **5**, 1205–1215 (1999).
7. R. N. Bryan, "In vivo morphologic imaging taken to a higher level," *Radiology* **254**, 647–650 (2010).
8. V. W. Lihong, "Tutorial on Photoacoustic Microscopy and Computed Tomography," *IEEE J. Sel. Top. Quantum Electron.* **14**, 171–179 (2008).
9. R. F. Bonner, R. Nossal, S. Havlin and G. H. Weiss, "Model for photon migration in turbid biological media," *J. Opt. Soc. Am.* **4**, 423–432 (1987).
10. A. H. Gandjbakhche and G. H. Weiss, "Random walk and diffusion-like models of photon migration in turbid media," *Prog. Optics* **34**, 333–402 (1995).
11. T. Durduran, A. G. Yodh, B. Chance, and D. A. Boas, "Does the photon-diffusion coefficient depend on absorption?," *J. Opt. Soc. Am. A* **14**, 3358–3365 (1997).
12. A. Amelink, H. J. C. Sterenborg, M. P. L. Bard, and S. A. Burgers, "In vivo measurement of the local optical properties of tissue by use of differential path-length spectroscopy," *Opt. Lett.* **29**, 1087–1089 (2004).
13. G. Zonios and A. Dimou, "Modeling diffuse reflectance from semi-infinite turbid media: application to the study of skin optical properties," *Opt. Express* **14**, 8661–8674 (2006).
14. R. Reif, O. A' Amar, and I. J. Bigio, "Analytical model of light reflectance for extraction of the optical properties in small volumes of turbid media," *Appl. Opt.* **46**, 7317–7328 (2007).
15. C. Billet and R. Sablong, "Differential optical spectroscopy for absorption characterization of scattering media," *Opt. Lett.* **32**, 3251–3253 (2007).
16. J. M. Schmitt, G. X. Zhou, E. C. Walker, and R. T. Wall, "Multi layer model of photon diffusion in skin," *J. Opt. Soc. Am. A* **7**, 2141–2153 (1990).
17. M. Shimada, C. Sato, Y. Hoshi, and Y. Yamada, "Estimation of the absorption coefficients of two-layered media by a simple method using spatially and time-resolved reflectances," *Phys. Med. Biol.* **54**, 5057–5071 (2009).
18. R. Nossal, J. Kiefer, G. H. Weiss, R. Bonner, H. Taitelbaum, and S. Havlin, "Photon migration in layered media," *Appl. Opt.* **27**, 3382–3391 (1988).
19. H. Taitelbaum, S. Havlin, and G. H. Weiss, "Approximate theory of photon migration in a 2-layer medium," *Appl. Opt.* **28**, 2245–2249 (1989).
20. I. Dayan, S. Havlin, and G. H. Weiss, "Photon migration in a two-layer turbid medium. A diffusion analysis," *J. Mod. Opt.* **39**, 1567–1582 (1992).
21. G. Alexandrakis, T. J. Farrell, and M. S. Patterson, "Accuracy of the diffusion approximation in determining the optical properties of a two-layer turbid medium," *Appl. Opt.* **37**, 7401–7409 (1998).
22. M. Das, C. Xu, and Q. Zhu, "Analytical solution for light propagation in a two-layer tissue structure with a tilted interface for breast imaging," *Appl. Opt.* **45**, 5027–5036 (2006).
23. A. D. Kim, C. Hayakawa, and V. Venugopalan, "Estimating optical properties in layered tissues by use of the Born approximation of the radiative transport equation," *Opt. Lett.* **31**, 1088–1090 (2006).
24. A. Kienle, M. S. Patterson, N. Dognitz, R. Bays, G. Wagnieres, and H. van den Bergh, "Noninvasive determination of the optical properties of two-layered turbid media," *Appl. Opt.* **37**, 779–791 (1998).
25. Q. Liu and N. Ramanujam, "Sequential estimation of optical properties of a two-layered epithelial tissue model from depth resolved ultraviolet-visible diffuse reflectance spectra," *Appl. Opt.* **45**, 4776–4790 (2006).
26. G. Mantis and G. Zonios, "Simple two-layer reflectance model for biological tissue applications," *Appl. Opt.* **48**, 3490–3496 (2009).
27. G. K. Reddy, "Photobiological basis and clinical role of low intensity lasers in biology and medicine," *J. Clin. Laser Med. Surg.* **22**, 141–150 (2004).
28. N. Ben Dov, G. Shefer, and A. Irintchev, "Low-energy laser irradiation affects satellite cell proliferation and differentiation in vitro," *Biochim. Biophys. Acta* **11**, 372–380 (1999).
29. M. Nitzan, A. Babchenko, B. Khanokh, and H. Taitelbaum, "Measurement of oxygen saturation in venous blood by dynamic near infrared spectroscopy," *J. Biomed. Opt.* **5**, 155–162 (2000).
30. J. S. Dam, C. B. Pedersen, T. Dalgaard, P. E. Fabricius, P. Aruna, and S. Andersson-Engels, "Fiber-optic probe for noninvasive real-time determination of tissue optical properties at multiple wavelengths," *Appl. Opt.* **40**, 1155–1164 (2001).
31. B. S. Suresh Anand and N. Sujatha, "Effects of intralipid-10% in fluorescence distortion studies on liquid-tissue phantoms in UV range," *J. Biophotonics* **4**, 92–97 (2011).
32. W. J. Wiscombe, "Mie scattering calculations: advances in technique and fast vector speed computer codes," *NCAR Technical Note NCAR/TN-140 + STR National Center for Atmospheric Research*, Boulder, Colorado (1979).
33. M. S. Patterson, E. Schwartz, and B. C. Wilson, "Quantitative reflectance spectrophotometry for the non-invasive measurement of photosensitizer concentration in tissue during photodynamic therapy," *Proc. SPIE* **1065**, 115–122 (1989).
34. A. Garcia-Urbe, E. B. Smith, J. Zou, M. Duvic, V. Prieto, and L. V. Wang, "In-vivo characterization of optical properties of pigmented skin lesions including melanoma using oblique incidence diffuse reflectance spectrometry," *J. Biomed. Opt.* **16**, 020501 (2011).